

# Efficient Fast Multipole Accelerated Boundary Elements via Recursive Computation of Multipole Expansions of Integrals

Nail A. Gumerov and Ramani Duraiswami

University of Maryland Institute for Advanced Computer Studies, College Park, MD 20742

---

## Abstract

In boundary element methods (BEM) in  $\mathcal{R}^3$ , matrix elements and right hand sides are typically computed via integration over line, triangle and tetrahedral volume elements. When the problem size gets large, the resulting linear systems are often solved iteratively via Krylov methods, with fast multipole methods (FMM) used to accelerate the matrix vector products needed. The integrals are often computed via numerical or analytical quadrature. When FMM acceleration is used, most entries of the matrix never need be computed explicitly - they are only needed in terms of their contribution to the multipole expansion coefficients. Furthermore, the two parts of this resulting algorithm - the integration and the FMM matrix vector product - are both approximate, and their errors have to be matched to avoid wasteful computations, or poorly controlled error. We propose a new fast method for generation of multipole expansion coefficients for the fields produced by the integration of the single and double layer potentials on surface triangles; charge distributions over line segments; and regular functions over tetrahedra in the volume; so that the overall method is well integrated into the FMM, with controlled error. The method is based on recursive computations of the multipole moments for  $O(1)$  cost per moment with a low asymptotic constant. The method is developed for the Laplace Green's function in  $\mathbb{R}^3$ . The derived recursions are tested both for accuracy and performance.

**Keywords:** Fast Multipole Method, Boundary Element Method, Multipole Expansions

---

## 1. Introduction

The fast multipole method (FMM) [5] is often used to accelerate the matrix vector products needed in the Krylov subspace based iterative methods for the solution of large linear systems that result from boundary element methods (BEM) (e.g., for a review see [12]). The surface is usually discretized via triangles, which for the lowest-order consistent approximation replaces the real boundary with a discretized version consisting of flat triangles, over which the functions of interest are approximated via low order polynomials. For constant panel methods, the BEM matrix elements can be represented as integrals of the Green's function and its derivatives over the triangles. In the Galerkin method of moments (MoM) a second integration is performed over the triangles [10].

The conventional BEM solution proceeds by evaluating all matrix elements via quadrature over the surface elements and solving the linear system either via matrix decomposition or iteratively. When used with the FMM accelerated iterative methods (FMMBEM), the matrix vector products are evaluated approximately, and these integrals are only needed as far as their elements contribute to the final product. While there exist methods to evaluate such integrals exactly or approximately with controlled accuracy (e.g., [2]), this approximation may not be consistent with that needed in the FMM. We need exact integrals for some elements (those in the near field) and for the others (in the far field) the integrals are only needed as far as their contribution to the consolidated far-field multipole expansions are concerned. Most previous work on

FMMBEM does not treat the problem consistently, either doing too much work in evaluating the integrals accurately, or alternately approximating them grossly, by only retaining the leading order monopole/dipole contributions.

Examples of works that do too much work in computing the multipole expansion coefficients (also known as multipole moments) based on their integral representations include [15] who use numerical quadrature, or [13] who do it analytically. These numerical and analytical evaluation procedures are quite expensive in three dimensions, as one may end up with the need to compute hundreds of integrals per triangle (as one may need to generate hundreds of the multipole moments per triangle), and may require tens of thousands of evaluations of the integrands per triangle (assuming that, of the order 100 quadrature points are used per triangle to satisfy the error bounds of the FMM). Furthermore, this step also needs to be done for field evaluations, where local expansions are used, as integration over the receiver triangles is needed (the local expansions have the same size as the multipole expansions).

There have been some alternate proposals for approaches that are numerically more compact. An example of such an approach is in [3], where the far field expansions for triangles are simply based on the expansions of equivalent monopoles and dipoles for the evaluation points separated from the source triangle by a sufficient cutoff distance. While this method can be tuned to improve the accuracy of the boundary element method approximation and geometrical errors, it loses the advantage the FMM has of consistent error control in all steps.

The focus of this paper is the development of quadrature formulae that produce multipole expansion coefficients consistent with the prescribed error bound, and ensuring that the computational and memory needs of the FMMBEM are optimal, thus developing a tightly integrated FMMBEM, whose cost per iteration is very close to the cost of a single evaluation of a FMM matrix vector product for isolated sources located at the panel centers of the BEM mesh. The method is presented for boundary integrals related to the Green's function for the Laplace equation, and is also applicable to the evaluation stage. These kernels appear in many application areas, including those for linear elasticity [14], viscosity [15], and low frequency electromagnetism [9], and the approach can be used in the FMM for a broad class of problems. The method is based on recursive computations, and requires  $O(1)$  operations (with low asymptotic constant) per multipole moment. Using the developed method, generation of the multipole expansions for the triangles requires about the same time as for generation of the multipole expansions for monopoles and dipoles, which is a significant improvement.

The BEM in  $\mathbb{R}^3$  is used to solve not only the Laplace equation with regular boundaries, but also in domains with filaments and wires (in vortex filament methods and for magnetostatics based on the Biot-Savart law, and for fields around electric wires). Further, when the equations being solved have a volume term, the internal volume needs to be discretized (via tetrahedral elements) and integrals taken over volume elements. All these need additional formulae for multipole coefficients from quadrature, which we provide.

We conducted accuracy and performance tests and integrated the method to our FMMBEM solver for the Laplace equation. The results of these tests are discussed in this paper. Using our approach we obtain a consistently accurate FMMBEM solver whose cost per iteration is very comparable to a simple FMM matrix vector product, that is with very small increase in cost for accurate quadrature.

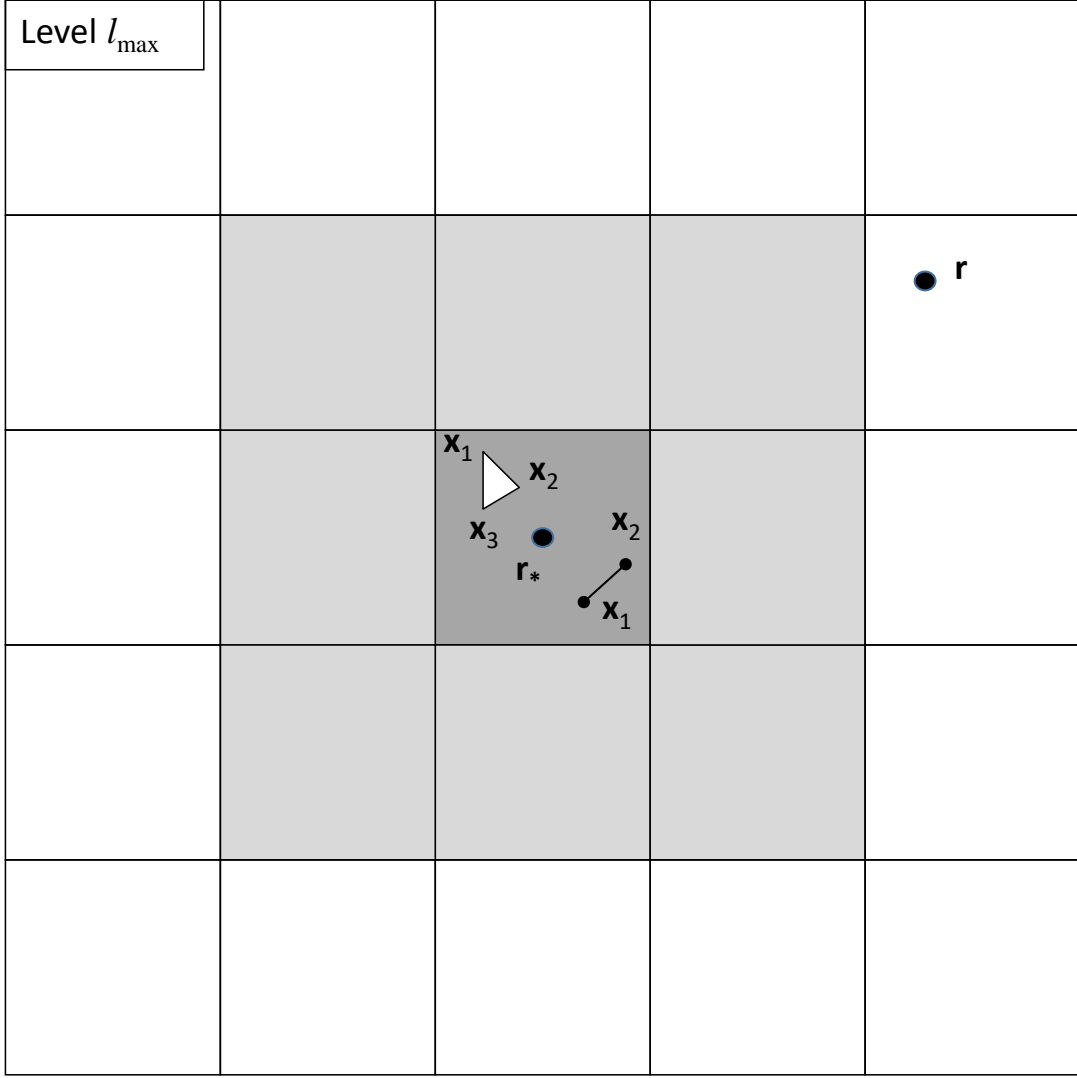


Figure 1: An illustrative sketch (in two-dimensions for clarity) of the problem geometry of the use of the FMM for matrix vector products. The finest level of the octree is shown with the source box (the darker shaded box), which contains simplices over which quadrature must be performed (only the line segment and triangle are shown) to achieve the matrix elements. A multipole expansion with origin at the box center needs to be generated for these elements, and should provide accurate representations of the integrals over the simplices to the specified accuracy, for any point  $\mathbf{r}$  outside the neighborhood of the source box (the lighter shaded region).

## 2. Problem Statement

In the BEM, as the surface  $S$  is discretized by triangles  $S_j$ ,  $j = 1, \dots, N$  the single and double layer potentials can be approximated as

$$\begin{aligned}
 L(\mathbf{r}) &= \int_S \sigma(\mathbf{r}') G(\mathbf{r}, \mathbf{r}') dS(\mathbf{r}') \approx \sum_{j=1}^N \sigma_j L_j(\mathbf{r}), \\
 M(\mathbf{r}) &= \int_S \sigma(\mathbf{r}') \frac{\partial G(\mathbf{r}, \mathbf{r}')}{\partial n(\mathbf{r}')} dS(\mathbf{r}') \approx \sum_{j=1}^N \sigma_j M_j(\mathbf{r}),
 \end{aligned} \tag{1}$$

where we accepted a constant panel approximation, so  $\sigma_j$  is the values of surface density at the  $j$ th triangle,  $G(\mathbf{r}, \mathbf{r}')$  is the Green function and  $L_j(\mathbf{r})$  and  $M_j(\mathbf{r})$  are the elementary integrals over the triangles,

$$\begin{aligned} L_j(\mathbf{r}) &= \int_{S_j} G(\mathbf{r}, \mathbf{r}') dS(\mathbf{r}'), \\ M_j(\mathbf{r}) &= \int_{S_j} \frac{\partial G(\mathbf{r}, \mathbf{r}')}{\partial n(\mathbf{r}')} dS(\mathbf{r}'), \\ G(\mathbf{r}, \mathbf{r}') &= \frac{1}{4\pi |\mathbf{r} - \mathbf{r}'|}. \end{aligned} \quad (2)$$

For given  $\sigma_j$  the integrals can be evaluated at any spatial point  $\mathbf{r}$  (either in the domain or on the surface). Moreover, the gradients of these potentials may also be needed if we need to compute domain derivatives, or are using the Maue identity.

A similar problem appears in magnetostatics and in vortex methods, where the Bio-Savart integral is in use, e.g.

$$\begin{aligned} \mathbf{H}(\mathbf{r}) &= \frac{1}{4\pi} \int_C \frac{\mathbf{I}(\mathbf{r}') \times (\mathbf{r} - \mathbf{r}')}{|\mathbf{r} - \mathbf{r}'|^3} dC(\mathbf{r}') \approx \nabla \times \sum_{j=1}^N \mathbf{I}_j K_j(\mathbf{r}), \\ K_j(\mathbf{r}) &= \int_{C_j} G(\mathbf{r}, \mathbf{r}') dl(\mathbf{r}'), \end{aligned} \quad (3)$$

where  $C$  is a single or multiple contours subdivided into  $N$  straight line segments (line elements)  $C_j$ ,  $j = 1, \dots, N$ ,  $\mathbf{I}$  is the current directed along the line element and represented by constants  $\mathbf{I}_j$  for each element.

Finally, we note that computation of volume integrals is a part of integral solution of the Poisson equation, as

$$\begin{aligned} N(\mathbf{r}) &= \int_V f(\mathbf{r}') G(\mathbf{r}, \mathbf{r}') dV(\mathbf{r}') \approx \sum_{j=1}^N f_j N_j(\mathbf{r}), \\ N_j(\mathbf{r}) &= \int_{V_j} G(\mathbf{r}, \mathbf{r}') dV(\mathbf{r}'), \end{aligned} \quad (4)$$

where we assume that the total volume  $V \subset \mathbb{R}^3$  is subdivided to tetrahedral finite elements  $V_j$  and a piecewise constant approximation is acceptable for  $f(\mathbf{r}')$ .

It is noticeable, that integrals  $K_j$ ,  $L_j$ ,  $M_j$ , and  $N_j$  be computed analytically (e.g., see [11]). However, for  $M$  evaluation points the complexity of such brute force computations is  $O(MN)$ . The FMM reduces this complexity to  $O(M + N)$ . While the FMM designed for summation of monopoles and dipoles of the Laplace equation can be used along with the correction factor matrices [3], a more efficient and integrated version would be obtained if it were possible to just modify the algorithm to directly generate the multipole expansions that evaluate to these integrals, namely,

$$F_j(\mathbf{r}) = \sum_{n=0}^{p-1} \sum_{m=-n}^n F_{jn}^m(\mathbf{r}_*) S_n^m(\mathbf{r} - \mathbf{r}_*) + R_p^{(F)}, \quad F = K, L, M, N. \quad (5)$$

where  $\mathbf{r}_*$  is the expansion center (the center of the smallest box in the octree containing the center of the  $j$ th surface or line element,  $\mathbf{r}_j$ , so the expansions are valid at  $|\mathbf{r} - \mathbf{r}_*| > |\mathbf{r}_j - \mathbf{r}_*|$ ),  $S_n^m$  are the spherical basis functions (multipoles) of the Laplace equation,  $p$  is the truncation number,  $K_{jn}^m$ ,  $L_{jn}^m$ ,  $M_{jn}^m$ , and  $N_{jn}^m$  are the expansion coefficients, and  $R_p^{(K)}$ ,  $R_p^{(L)}$ ,  $R_p^{(M)}$ , and  $R_p^{(N)}$  are the residuals due to the truncation of infinite

series. The problem then is to create a method for fast generation of these coefficients. In the solution provided below, we propose a recursive process, which results in  $O(1)$  complexity per expansion coefficient with a low asymptotic constant. Note that this process can be used also at the evaluation stage for Galerkin method of moments, which we elaborate in discussion at the end of the paper.

Figure 1 provides a sketch of the problem geometry. Here, on the same figure a triangle and a line segment are shown (one can also add a tetrahedron). One can also see a box (the source box) of the octree they belong to. The center of the box is the center of the expansion, which should be valid at any point  $\mathbf{r}$  outside the neighborhood of the source box.

### 3. Solution

#### 3.1. Mappings

First, let us parameterize the volume, surface, and line elements considered using parameters  $(u, v, w)$ ,  $(u, v)$ , and  $u$  for the volume, surface, and line, respectively. Equations for the line and plane, and for points in the volume are

$$\begin{aligned} \mathbf{r} &= \mathbf{R}(u) = \mathbf{R}_u u + \mathbf{R}_0 \quad (\text{line}), \\ \mathbf{r} &= \mathbf{R}(u, v) = \mathbf{R}_u u + \mathbf{R}_v v + \mathbf{R}_0 \quad (\text{plane}), \\ \mathbf{r} &= \mathbf{R}(u, v, w) = \mathbf{R}_u u + \mathbf{R}_v v + \mathbf{R}_w w + \mathbf{R}_0 \quad (\text{space}), \end{aligned} \quad (6)$$

where  $\mathbf{r}$  is the radius-vector of a point, while  $\mathbf{R}_u, \mathbf{R}_v, \mathbf{R}_w$ , and  $\mathbf{R}_0$  are constant vectors in  $\mathbb{R}^3$ . Such parametrization also provides mapping of arbitrary line segments, triangles, and tetrahedrons on standard simplices, which can be selected as a unit segment with end points at  $u = 0$  and  $u = 1$ , rectangular triangle,  $T$ , with vertices  $(0, 0), (1, 0)$ , and  $(0, 1)$  in  $(u, v)$ -plane, and tri-rectangular tetrahedron,  $Q$ , with vertices  $(0, 0, 0), (1, 0, 0), (0, 1, 0)$ , and  $(0, 0, 1)$  in  $(u, v, w)$ -space.

The correspondence of the vertices of the elements, which are points  $\mathbf{x}_1$  and  $\mathbf{x}_2$ , for a segment, points  $\mathbf{x}_1, \mathbf{x}_2$ , and  $\mathbf{x}_3$  for a triangle, and  $\mathbf{x}_1, \mathbf{x}_2, \mathbf{x}_3$ , and  $\mathbf{x}_4$  for a tetrahedron, provides a unique mapping, i.e., vectors  $\mathbf{R}_u, \mathbf{R}_v, \mathbf{R}_w$ , and  $\mathbf{R}_0$ . Indeed, we have

$$\begin{aligned} \mathbf{x}_1 &= \mathbf{R}(0) = \mathbf{R}_0, \quad \mathbf{x}_2 = \mathbf{R}(1) = \mathbf{R}_u + \mathbf{R}_0 \quad (\text{segment}), \\ \mathbf{x}_1 &= \mathbf{R}(0, 0) = \mathbf{R}_0, \quad \mathbf{x}_2 = \mathbf{R}(1, 0) = \mathbf{R}_u + \mathbf{R}_0, \quad \mathbf{x}_3 = \mathbf{R}(0, 1) = \mathbf{R}_v + \mathbf{R}_0 \quad (\text{triangle}), \\ \mathbf{x}_1 &= \mathbf{R}(0, 0, 0) = \mathbf{R}_0, \quad \mathbf{x}_2 = \mathbf{R}(1, 0, 0) = \mathbf{R}_u + \mathbf{R}_0 \quad (\text{tetrahedron}), \\ \mathbf{x}_3 &= \mathbf{R}(0, 1, 0) = \mathbf{R}_v + \mathbf{R}_0, \quad \mathbf{x}_4 = \mathbf{R}(0, 0, 1) = \mathbf{R}_w + \mathbf{R}_0 \quad (\text{tetrahedron}). \end{aligned} \quad (7)$$

Hence, given coordinates of the vertices, we can determine

$$\mathbf{R}_0 = \mathbf{x}_1, \quad \mathbf{R}_u = \mathbf{x}_2 - \mathbf{x}_1, \quad \mathbf{R}_v = \mathbf{x}_3 - \mathbf{x}_1, \quad \mathbf{R}_w = \mathbf{x}_4 - \mathbf{x}_1 \quad (8)$$

where  $\mathbf{R}_w$  is defined only for the tetrahedron and  $\mathbf{R}_v$  for the triangle and tetrahedron. This transform shows also that

$$\begin{aligned} L_j &= J^{(j)} \int_T G(\mathbf{r}, \mathbf{R}^{(j)}(u, v)) dS(u, v), \quad J^{(j)} = |\mathbf{R}_u^{(j)} \times \mathbf{R}_v^{(j)}|, \\ M_j &= J^{(j)} \int_T \frac{\partial}{\partial n_j} G(\mathbf{r}, \mathbf{R}^{(j)}(u, v)) dS(u, v), \\ K_j &= J^{(j)} \int_0^1 G(\mathbf{r}, \mathbf{R}^{(j)}(u)) du, \quad J^{(j)} = |\mathbf{R}_u^{(j)}|, \\ N_j &= J^{(j)} \int_Q G(\mathbf{r}, \mathbf{R}^{(j)}(u, v, w)) dV(u, v, w), \quad J^{(j)} = |(\mathbf{R}_u^{(j)} \times \mathbf{R}_v^{(j)}) \cdot \mathbf{R}_w^{(j)}|, \end{aligned} \quad (9)$$

where  $J^{(j)}$  is the Jacobian of transform of the  $j$ th simplex to the standard simplex.

### 3.2. Basis functions

The spherical basis functions satisfying the Laplace equation typically used in the fast multipole method, are the singular basis functions at the origin of the reference frame (multipoles),  $S_n^m(\mathbf{r})$ , and regular basis functions, or harmonic polynomials,  $R_n^m(\mathbf{r})$ . These can be expressed via spherical harmonics, and may have different normalization. We accept the following definition:

$$\begin{aligned} R_n^m(\mathbf{r}) &= \frac{(-1)^n i^{|m|}}{(n+|m|)!} r^n P_n^{|m|}(\cos \theta) e^{im\varphi}, \\ S_n^m(\mathbf{r}) &= i^{-|m|} (n-|m|)! r^{-n-1} P_n^{|m|}(\cos \theta) e^{im\varphi}, \\ n &= 0, 1, 2, \dots, \quad m = -n, \dots, n, \\ R_n^m(\mathbf{r}) &\equiv S_n^m(\mathbf{r}) \equiv 0, \quad |m| > n, \\ \mathbf{r} &= (x, y, z) = r (\sin \theta \cos \varphi, \sin \theta \sin \varphi, \cos \theta) \end{aligned} \quad (10)$$

where  $(r, \theta, \varphi)$  are the spherical coordinates of spatial point  $\mathbf{r}$ , and  $P_n^m$  are the associated Legendre functions, defined by the Rodrigues formula (see [1]),

$$P_n^m(\mu) = \frac{(-1)^m (1-\mu^2)^{m/2}}{2^n n!} \frac{d^{m+n}}{d\mu^{m+n}} (\mu^2 - 1)^n, \quad n \geq 0, \quad m \geq 0. \quad (11)$$

Note that the basis functions obey the following symmetry,

$$R_n^{-m}(\mathbf{r}) = (-1)^m \overline{R_n^m(\mathbf{r})}, \quad S_{(1)n}^{-m}(\mathbf{r}) = (-1)^m \overline{S_n^m(\mathbf{r})}, \quad (12)$$

where the bar indicates the complex conjugate. This shows that they can be computed only for non-negative  $m$ .

In these bases the Green's function can be expanded as

$$G(\mathbf{r}, \mathbf{r}') = \frac{1}{4\pi} \sum_{n=0}^{\infty} \sum_{m=-n}^n (-1)^n R_n^{-m}(\mathbf{r}' - \mathbf{r}_*) S_n^m(\mathbf{r} - \mathbf{r}_*), \quad |\mathbf{r} - \mathbf{r}_*| > R_0 > |\mathbf{r}' - \mathbf{r}_*|. \quad (13)$$

Comparing this with equations (2)-(5), we can see that

$$\begin{aligned} L_{jn}^m(\mathbf{r}_*) &= \frac{1}{4\pi} (-1)^n \int_{S_j} R_n^{-m}(\mathbf{r}' - \mathbf{r}_*) dS(\mathbf{r}'), \\ M_{jn}^m(\mathbf{r}_*) &= \frac{1}{4\pi} (-1)^n \mathbf{n}_j \cdot \int_{S_j} \nabla R_n^{-m}(\mathbf{r}' - \mathbf{r}_*) dS(\mathbf{r}'), \\ K_{jn}^m(\mathbf{r}_*) &= \frac{1}{4\pi} (-1)^n \int_{C_j} R_n^{-m}(\mathbf{r}' - \mathbf{r}_*) dC(\mathbf{r}'), \\ N_{jn}^m(\mathbf{r}_*) &= \frac{1}{4\pi} (-1)^n \int_{V_j} R_n^{-m}(\mathbf{r}' - \mathbf{r}_*) dV(\mathbf{r}'), \end{aligned} \quad (14)$$

where  $\mathbf{n}_j$  is the normal to the  $j$ th surface element. The following derivatives of the harmonic polynomials are also harmonic polynomials, as the following relations hold (e.g., see [6]),

$$\begin{aligned} \frac{\partial}{\partial z} R_n^m(\mathbf{r}) &= -R_{n-1}^m(\mathbf{r}), \\ \frac{\partial}{\partial \eta} R_n^m(\mathbf{r}) &= i R_{n-1}^{m+1}(\mathbf{r}), \\ \frac{\partial}{\partial \xi} R_n^m(\mathbf{r}) &= i R_{n-1}^{m-1}(\mathbf{r}), \end{aligned} \quad (15)$$

where

$$\xi = \frac{x + iy}{2}, \quad \eta = \frac{x - iy}{2}; \quad x = \xi + \eta, \quad y = -i(\xi - \eta). \quad (16)$$

and

$$\frac{\partial}{\partial \eta} = \frac{\partial}{\partial x} + i \frac{\partial}{\partial y}, \quad \frac{\partial}{\partial \xi} \equiv \frac{\partial}{\partial x} - i \frac{\partial}{\partial y}. \quad (17)$$

Thus, we have

$$\mathbf{n} \cdot \nabla R_n^m(\mathbf{r}) = in_x [R_{n-1}^{m+1}(\mathbf{r}) + R_{n-1}^{m-1}(\mathbf{r})] + n_y [R_{n-1}^{m+1}(\mathbf{r}) - R_{n-1}^{m-1}(\mathbf{r})] - n_z R_{n-1}^m(\mathbf{r}), \quad (18)$$

where  $\mathbf{n} = (n_x, n_y, n_z)$ . This shows that computation of all integrals can be reduced to computation of elementary integrals

$$\begin{aligned} a_{jn}^m &= \int_Q c_{jn}^m(u, v, w) dS(u, v) = \int_0^1 \int_0^{1-u} \int_0^{1-u-v} c_{jn}^m(u, v, w) dw dv du, \\ c_{jn}^m(u, v, w) &= R_n^m(\mathbf{R}^{(j)}(u, v, w) - \mathbf{r}_*), \\ i_{jn}^m &= \int_T g_{jn}^m(u, v) dS(u, v) = \int_0^1 \int_0^{1-u} g_{jn}^m(u, v) dv du, \quad g_{jn}^m(u, v) = R_n^m(\mathbf{R}^{(j)}(u, v) - \mathbf{r}_*), \\ p_{jn}^m &= \int_0^1 r_{jn}^m(u) du, \quad r_{jn}^m(u) = R_n^m(\mathbf{R}^{(j)}(u) - \mathbf{r}_*). \end{aligned} \quad (19)$$

The expansion coefficients then can be found as

$$\begin{aligned} K_{jn}^m &= \frac{(-1)^n J^{(j)}}{4\pi} p_{jn}^{-m}, \quad L_{jn}^m = \frac{(-1)^n J^{(j)}}{4\pi} i_{jn}^{-m}, \quad M_{jn}^m = \frac{(-1)^n J^{(j)}}{4\pi} l_{jn}^{-m}, \quad N_{jn}^m = \frac{J^{(j)}}{4\pi} (-1)^n a_{jn}^m, \\ l_{jn}^{-m} &= in_x [i_{j,n-1}^{-m+1} + i_{j,n-1}^{-m-1}] + n_y [i_{j,n-1}^{-m+1} - i_{j,n-1}^{-m-1}] - n_z i_{j,n-1}^{-m}. \end{aligned} \quad (20)$$

### 3.3. Integration lemmas

Below we are going to prove a few integration lemmas related to integrals (19). To simplify notation we drop there subscript/superscript  $j$  as a notion of the  $j$ th triangle. Furthermore, we accept simplification  $\mathbf{r}_* = \mathbf{0}$ . Generally, according Eq. (6), we have

$$\begin{aligned} \mathbf{R}(u) - \mathbf{r}_* &= \mathbf{R}_u u + \mathbf{R}_0 - \mathbf{r}_* \quad (line), \\ \mathbf{R}(u, v) - \mathbf{r}_* &= \mathbf{R}_u u + \mathbf{R}_v v + \mathbf{R}_0 - \mathbf{r}_* \quad (plane), \\ \mathbf{R}(u, v, w) - \mathbf{r}_* &= \mathbf{R}_u u + \mathbf{R}_v v + \mathbf{R}_w w + \mathbf{R}_0 - \mathbf{r}_* \quad (space), \end{aligned} \quad (21)$$

So, one can easily avoid this simplification by correcting parameter  $\mathbf{R}_0$ .

Also, we note that  $R_n^m$  are homogeneous polynomials of degree  $n$  of arguments  $(x, y, z)$  or  $(\xi, \eta, z)$ . Hence, according to the Euler's theorem on homogeneous functions we have

$$n R_n^m(\mathbf{r}) = \xi \frac{\partial R_n^m(\mathbf{r})}{\partial \xi} + \eta \frac{\partial R_n^m(\mathbf{r})}{\partial \eta} + z \frac{\partial R_n^m(\mathbf{r})}{\partial z}. \quad (22)$$

Substituting here differential relations (15), we obtain

$$n R_n^m(\mathbf{r}) = i \xi R_{n-1}^{m-1}(\mathbf{r}) + i \eta R_{n-1}^{m+1}(\mathbf{r}) - z R_{n-1}^m(\mathbf{r}). \quad (23)$$

Furthermore, according to Eq. (6) for the points in space, we have

$$\begin{aligned}\xi(u, v, w) &= \xi_u u + \xi_v v + \xi_w w + \xi_0, \\ \eta(u, v, w) &= \eta_u u + \eta_v v + \eta_w w + \eta_0, \\ z(u, v, w) &= z_u u + z_v v + z_w w + z_0,\end{aligned}\tag{24}$$

For points on a surface or a line we have the same relations, where the dependence on parameter  $w$  should be neglected ( $\xi_w = \eta_w = z_w = 0$ ). Also, for points on the line we have ( $\xi_v = \eta_v = z_v = 0$ ).

**Lemma 1 (1).** *The following recursion holds for  $p_n^m$  defined by Eq. (19)*

$$p_n^m = \frac{1}{n+1} [i\xi_0 p_{n-1}^{m-1} + i\eta_0 p_{n-1}^{m+1} - z_0 p_{n-1}^m + q_n^m], \quad q_n^m = r_n^m(1).\tag{25}$$

**Proof.** Due to relations (15), (23), and (24) at  $\xi_v = \eta_v = z_v = 0$  we have

$$\begin{aligned}u \frac{\partial r_n^m}{\partial u} &= \xi_u u \frac{\partial R_n^m}{\partial \xi} + z_u u \frac{\partial R_n^m}{\partial z} \\ &= \xi \frac{\partial R_n^m}{\partial \xi} + \eta \frac{\partial R_n^m}{\partial \eta} + z \frac{\partial R_n^m}{\partial z} - \left( \xi_0 \frac{\partial R_n^m}{\partial \xi} + \eta_0 \frac{\partial R_n^m}{\partial \eta} + z_0 \frac{\partial R_n^m}{\partial z} \right) \\ &= nr_n^m - (i\xi_0 r_{n-1}^{m-1} + i\eta_0 r_{n-1}^{m+1} - z_0 r_{n-1}^m).\end{aligned}$$

This shows that

$$\int_0^1 u \frac{\partial r_n^m}{\partial u} du = np_n^m - (i\xi_0 p_{n-1}^{m-1} + i\eta_0 p_{n-1}^{m+1} - z_0 p_{n-1}^m).$$

On the other hand, integration by parts results in

$$\int_0^1 u \frac{\partial r_n^m}{\partial u} du = \int_0^1 u dr_n^m = r_n^m(1) - \int_0^1 r_n^m du = q_n^m - p_n^m.$$

Comparing these expressions we obtain the statement of the lemma. End of proof. ■

**Lemma 2 (2).** *The following recursion holds for  $i_n^m$  defined in Eq. (19),*

$$i_n^m = \frac{1}{n+2} (i\xi_0 i_{n-1}^{m-1} + i\eta_0 i_{n-1}^{m+1} - z_0 i_{n-1}^m + j_n^m),\tag{26}$$

where

$$j_n^m = \int_0^1 h_n^m(u) du, \quad h_n^m(u) = g_n^m(u, 1-u).\tag{27}$$

**Proof.** Due to relations (15), (23), and (24) we have

$$\begin{aligned}u \frac{\partial g_n^m}{\partial u} + v \frac{\partial g_n^m}{\partial v} &= (\xi_u u + \xi_v v) \frac{\partial R_n^m}{\partial \xi} + (\eta_u u + \eta_v v) \frac{\partial R_n^m}{\partial \eta} + (z_u u + z_v v) \frac{\partial R_n^m}{\partial z} \\ &= \xi \frac{\partial R_n^m}{\partial \xi} + \eta \frac{\partial R_n^m}{\partial \eta} + z \frac{\partial R_n^m}{\partial z} - \left( \xi_0 \frac{\partial R_n^m}{\partial \xi} + \eta_0 \frac{\partial R_n^m}{\partial \eta} + z_0 \frac{\partial R_n^m}{\partial z} \right) \\ &= ng_n^m - (i\xi_0 g_{n-1}^{m-1} + i\eta_0 g_{n-1}^{m+1} - z_0 g_{n-1}^m).\end{aligned}\tag{28}$$



This shows that

$$\int_T \left( u \frac{\partial g_n^m}{\partial u} + v \frac{\partial g_n^m}{\partial v} \right) dS = n i_n^m - (i \xi_0 i_{n-1}^{m-1} + i \eta_0 i_{n-1}^{m+1} - z_0 i_{n-1}^m). \quad (29)$$

On the other hand, this integral can be computed as follows

$$\begin{aligned} \int_T \left( u \frac{\partial g_n^m}{\partial u} + v \frac{\partial g_n^m}{\partial v} \right) dS &= \int_0^1 \int_0^{1-v} u \frac{\partial g_n^m}{\partial u} du dv + \int_0^1 \int_0^{1-u} v \frac{\partial g_n^m}{\partial v} dv du \\ &= \int_0^1 \int_0^{1-v} u (d_u g_n^m) dv + \int_0^1 \int_0^{1-u} v (d_v g_n^m) du \\ &= \int_0^1 \left[ u g_n^m|_0^{1-v} - \int_0^{1-v} g_n^m du \right] dv + \int_0^1 \left[ v g_n^m|_0^{1-u} - \int_0^{1-u} g_n^m dv \right] du \\ &= \int_0^1 [(1-v) g_n^m(1-v, v)] dv + \int_0^1 [(1-u) g_n^m(u, 1-u)] du - 2 \int_T g_n^m dS \\ &= \int_0^1 g_n^m(u, 1-u) du - 2 i_n^m, \end{aligned} \quad (30)$$

where the last equality can be checked by substitution of variable  $v = 1 - u$  in the integral over  $v$ ,

$$\begin{aligned} &\int_0^1 [(1-v) g_n^m(1-v, v)] dv + \int_0^1 [(1-u) g_n^m(u, 1-u)] du \\ &= \int_0^1 [u g_n^m(u, 1-u)] du + \int_0^1 [(1-u) g_n^m(u, 1-u)] du = \int_0^1 g_n^m(u, 1-u) du. \end{aligned} \quad (31)$$

Equalizing expressions Eq. (29) and (30) we obtain

$$\int_0^1 g_n^m(u, 1-u) du - 2 \int_T g_n^m dS = n \int_T g_n^m dS - \left( i \xi_0 \int_T g_{n-1}^{m-1} dS + i \eta_0 \int_T g_{n-1}^{m+1} dS - z_0 \int_T g_{n-1}^m dS \right).$$

This is equivalent to the statement of the lemma (26). End of proof. ■

**Lemma 3 (3).** *The following recursion holds for  $j_n^m$  defined by Eq. (27)*

$$j_n^m = \frac{1}{n+1} [i(\xi_0 + \xi_v) j_{n-1}^{m-1} + i(\eta_0 + \eta_v) j_{n-1}^{m+1} - (z_0 + z_v) j_{n-1}^m + k_n^m], \quad k_n^m = g_n^m(1, 0). \quad (32)$$

**Proof.** Note that at  $\mathbf{r}_* = \mathbf{0}$  the integrand in Eq. (27) is

$$\begin{aligned} h_n^m(u) &= g_n^m(u, 1-u) = R_n^m(\mathbf{R}(u, 1-u)) \\ &= R_n^m(\mathbf{R}_u u + \mathbf{R}_v(1-u) + \mathbf{R}_0) = R_n^m((\mathbf{R}_u - \mathbf{R}_v)u + \mathbf{R}_v + \mathbf{R}_0). \end{aligned} \quad (33)$$

This is the same as  $r_n^m(u)$  for the line integral, but with  $\mathbf{R}_u - \mathbf{R}_v$  instead of  $u$  and  $\mathbf{R}_v + \mathbf{R}_0$  instead of  $\mathbf{R}_0$ . From Lemma 1 (Eq. 25) we obtain the statement of the lemma by replacing  $\xi_0, \eta_0$ , and  $z_0$  with  $\xi_0 + \xi_v, \eta_0 + \eta_v$ , and  $z_0 + z_v$ . We also note that  $q_n^m$  there corresponds to  $k_n^m$  since at  $u = 1$  we have  $g_n^m(1, 0) = r_n^m(1) = R_n^m(\mathbf{R}_u + \mathbf{R}_0)$ . End of proof. ■

**Lemma 4 (4).** *The following recursion holds for  $b_n^m$  defined in Eq. (19),*

$$a_n^m = \frac{1}{n+3} (i \xi_0 a_{n-1}^{m-1} + i \eta_0 a_{n-1}^{m+1} - z_0 a_{n-1}^m + b_n^m), \quad (34)$$

where

$$b_n^m = \int_0^1 \int_0^{1-v} d_n^m(u, v) du dv, \quad d_n^m(u, v) = c_n^m(u, v, 1-u-v). \quad (35)$$

**Proof.** Due to relations (15), (23), and (24) we have

$$\begin{aligned}
& u \frac{\partial c_n^m}{\partial u} + v \frac{\partial c_n^m}{\partial v} + w \frac{\partial c_n^m}{\partial w} \\
&= (\xi_u u + \xi_v v + \xi_w w) \frac{\partial R_n^m}{\partial \xi} + (\eta_u u + \eta_v v + \eta_w w) \frac{\partial R_n^m}{\partial \eta} + (z_u u + z_v v + z_w w) \frac{\partial R_n^m}{\partial z} \\
&= \xi \frac{\partial R_n^m}{\partial \xi} + \eta \frac{\partial R_n^m}{\partial \eta} + z \frac{\partial R_n^m}{\partial z} - \left( \xi_0 \frac{\partial R_n^m}{\partial \xi} + \eta_0 \frac{\partial R_n^m}{\partial \eta} + z_0 \frac{\partial R_n^m}{\partial z} \right) \\
&= n c_n^m - (i \xi_0 c_{n-1}^{m-1} + i \eta_0 c_{n-1}^{m+1} - z_0 c_{n-1}^m).
\end{aligned} \tag{36}$$

So,

$$\int_Q \left( u \frac{\partial c_n^m}{\partial u} + v \frac{\partial c_n^m}{\partial v} + w \frac{\partial c_n^m}{\partial w} \right) dV = n a_n^m - (i \xi_0 a_{n-1}^{m-1} + i \eta_0 a_{n-1}^{m+1} - z_0 a_{n-1}^m). \tag{37}$$

Integral of the left hand side of (37) over the standard tetrahedron can be represented as

$$\begin{aligned}
& \int_Q \left( u \frac{\partial c_n^m}{\partial u} + v \frac{\partial c_n^m}{\partial v} + w \frac{\partial c_n^m}{\partial w} \right) dV \\
&= \int_0^1 \int_0^{1-v} \int_0^{1-v-w} u \frac{\partial c_n^m}{\partial u} du dv dw + \int_0^1 \int_0^{1-w} \int_0^{1-u-w} v \frac{\partial c_n^m}{\partial v} dv du dw + \int_0^1 \int_0^{1-u} \int_0^{1-u-v} w \frac{\partial c_n^m}{\partial w} dw dv du \\
&= \int_0^1 \int_0^{1-v} \left[ u c_n^m \Big|_0^{1-v-w} - \int_0^{1-v-w} c_n^m du \right] dw dv + \int_0^1 \int_0^{1-w} \left[ v c_n^m \Big|_0^{1-u-w} - \int_0^{1-u-w} c_n^m dv \right] du dw \\
&\quad + \int_0^1 \int_0^{1-v} \left[ w c_n^m \Big|_0^{1-u-v} - \int_0^{1-u-v} c_n^m dw \right] du dv \\
&= \int_0^1 \int_0^{1-v} [(1-v-w) c_n^m(1-v-w, v, w)] dw dv + \int_0^1 \int_0^{1-w} [(1-u-w) c_n^m(u, 1-u-w, w)] du dw \\
&\quad + \int_0^1 \int_0^{1-v} [(1-u-v) c_n^m(u, v, 1-u-v)] dv du - 3 \int_Q c_n^m dV \\
&= \int_0^1 \int_0^{1-v} c_n^m(u, v, 1-u-v) du dv - 3 \int_Q c_n^m dV.
\end{aligned}$$

where the last identity can be checked by substitution  $w = 1 - u - v$  for integrals over  $w$  (at fixed  $v$  for the first and at fixed  $u$  for the second integral). Equalizing the last expression with Eq. (37) we obtain the statement of the lemma. End of proof.

**Lemma 5 (5).** *The following recursion holds for  $b_n^m$  defined by Eq. (35)*

$$\begin{aligned}
b_n^m &= \frac{1}{n+2} (i(\xi_0 + \xi_w) b_{n-1}^{m-1} + i(\eta_0 + \eta_w) b_{n-1}^{m+1} - (z_0 + z_w) b_{n-1}^m + e_n^m), \\
e_n^m &= \frac{1}{n+1} [i(\xi_0 + \xi_v) e_{n-1}^{m-1} + i(\eta_0 + \eta_v) e_{n-1}^{m+1} - (z_0 + z_v) e_{n-1}^m + f_n^m], \quad f_n^m = c_n^m(1, 0, 0).
\end{aligned} \tag{38}$$

■

**Proof.** Note that at  $\mathbf{r}_* = \mathbf{0}$  the integrand in Eq. (35) is

$$\begin{aligned}
d_n^m(u, v) &= c_n^m(u, v, 1-u-v) = R_n^m(\mathbf{R}(u, v, 1-u-v)) \\
&= R_n^m(\mathbf{R}_u u + \mathbf{R}_v v + \mathbf{R}_w(1-u-v) + \mathbf{R}_0) \\
&= R_n^m((\mathbf{R}_u - \mathbf{R}_w)u + (\mathbf{R}_v - \mathbf{R}_w)v + \mathbf{R}_w + \mathbf{R}_0).
\end{aligned} \tag{39}$$

This is the same as  $g_n^m(u, v)$  for the surface integral, but with  $\mathbf{R}_u - \mathbf{R}_w$ ,  $\mathbf{R}_v - \mathbf{R}_w$ , and  $\mathbf{R}_0 + \mathbf{R}_w$  instead of  $\mathbf{R}_u$ ,  $\mathbf{R}_v$ , and  $\mathbf{R}_0$ . Hence, the statement of this lemma is a corollary of Lemma (2) and Lemma (3) since  $f_n^m = c_n^m(1, 0, 0) = g_n^m(1, 0) = r_n^m(1) = R_n^m(\mathbf{R}_u + \mathbf{R}_0)$ . End of proof. ■

### 3.4. Recursions

Lemmas 1-5 along with relation (23) deliver a recursive method to compute all integrals  $p_n^m$ ,  $i_n^m$ , and  $a_n^m$ . Also auxiliary integrals  $j_n^m$ ,  $e_n^m$ , and  $b_n^m$  should also be computed recursively. Separate recursions are needed for  $q_n^m$ ,  $k_n^m$ , and  $f_n^m$ . Since

$$\begin{aligned} q_n^m &= r_n^m(1) = g_n^m(1, 0) = c_n^m(1, 0, 0) = k_n^m = f_n^m \\ &= R_n^m(\xi_u + \xi_0, \eta_u + \eta_0, z_u + z_0) \end{aligned} \quad (40)$$

we obtain from Eq. (23)

$$q_n^m = \frac{1}{n} [i(\xi_0 + \xi_u) q_{n-1}^{m-1} + i(\eta_0 + \eta_u) q_{n-1}^{m+1} - (z_0 + z_u) q_{n-1}^m]. \quad (41)$$

We note also that  $j_n^m$  and  $e_n^m$  satisfy the same recursions with the same initial values. So, that quantities are simply the same.

Note that in all recursions  $a_n^m, b_n^m, i_n^m, j_n^m$ , and  $q_n^m$  should be set to zero for  $|m| > n$ . This simply follows from definition of these quantities and the fact that  $R_n^m(\mathbf{r}) \equiv 0$  for  $|m| > n$ . This means that all functions of degree  $n$  can be obtained from functions of degree  $n - 1$ . The starting values for the recursions can be computed directly, since  $R_0^0 \equiv 1$ , and so

$$\begin{aligned} q_0^0 &= R_0^0 = 1, \\ p_0^0 &= j_0^0 = \int_0^1 R_0^0 du = 1, \\ i_0^0 &= b_0^0 = \int_0^1 \int_0^{1-u} R_0^0 dv du = \frac{1}{2}, \\ a_0^0 &= \int_0^1 \int_0^{1-u} \int_0^{1-u-v} R_0^0 dv du dw = \frac{1}{6}. \end{aligned} \quad (42)$$

Summarizing, we obtained the following recursions for the line integrals,

$$\begin{aligned} q_n^m &= \frac{1}{n} [i(\xi_0 + \xi_u) q_{n-1}^{m-1} + i(\eta_0 + \eta_u) q_{n-1}^{m+1} - (z_0 + z_u) q_{n-1}^m], \\ p_n^m &= \frac{1}{n+1} [i\xi_0 p_{n-1}^{m-1} + i\eta_0 p_{n-1}^{m+1} - z_0 p_{n-1}^m + q_n^m], \quad n = 1, 2, \dots \end{aligned} \quad (43)$$

The surface integrals can be computed using relations

$$\begin{aligned} q_n^m &= \frac{1}{n} [i(\xi_0 + \xi_u) q_{n-1}^{m-1} + i(\eta_0 + \eta_u) q_{n-1}^{m+1} - (z_0 + z_u) q_{n-1}^m], \\ j_n^m &= \frac{1}{n+1} [i(\xi_0 + \xi_v) j_{n-1}^{m-1} + i(\eta_0 + \eta_v) j_{n-1}^{m+1} - (z_0 + z_v) j_{n-1}^m + q_n^m], \\ i_n^m &= \frac{1}{n+2} (i\xi_0 i_{n-1}^{m-1} + i\eta_0 i_{n-1}^{m+1} - z_0 i_{n-1}^m + j_n^m), \quad n = 1, 2, \dots \end{aligned} \quad (44)$$

For the volume integrals we have

$$\begin{aligned}
q_n^m &= \frac{1}{n} [i(\xi_0 + \xi_u) q_{n-1}^{m-1} + i(\eta_0 + \eta_u) q_{n-1}^{m+1} - (z_0 + z_u) q_{n-1}^m], \\
j_n^m &= \frac{1}{n+1} [i(\xi_0 + \xi_v) j_{n-1}^{m-1} + i(\eta_0 + \eta_v) j_{n-1}^{m+1} - (z_0 + z_v) j_{n-1}^m + q_n^m], \\
b_n^m &= \frac{1}{n+2} [i(\xi_0 + \xi_w) b_{n-1}^{m-1} + i(\eta_0 + \eta_w) b_{n-1}^{m+1} - (z_0 + z_w) b_{n-1}^m + j_n^m], \\
a_n^m &= \frac{1}{n+3} (i\xi_0 a_{n-1}^{m-1} + i\eta_0 a_{n-1}^{m+1} - z_0 a_{n-1}^m + b_n^m), \quad n = 1, 2, \dots
\end{aligned} \tag{45}$$

Note then, that some other bases and symmetries can be exploited to make computations more efficient. For example, in [7] the entire FMM was implemented using the real basis functions defined as

$$\underline{R}_n^m = \begin{cases} \text{Re} \{ \tilde{R}_n^m \}, & m \geq 0, \\ \text{Im} \{ \tilde{R}_n^m \}, & m < 0 \end{cases}, \quad \underline{S}_n^m = \begin{cases} \text{Re} \{ \tilde{S}_n^m \}, & m \geq 0, \\ \text{Im} \{ \tilde{S}_n^m \}, & m < 0 \end{cases}, \tag{46}$$

where the complex valued basis functions with tildes are related to functions (10) via

$$\tilde{R}_n^m(\mathbf{r}) = i^{|m|} R_n^m(\mathbf{r}), \quad \tilde{S}_n^m(\mathbf{r}) = i^{-|m|} S_n^m(\mathbf{r}). \tag{47}$$

The functions obey the following symmetry

$$\tilde{R}_n^{-m}(\mathbf{r}) = \overline{\tilde{R}_n^m(\mathbf{r})}, \quad \tilde{S}_n^{-m}(\mathbf{r}) = \overline{\tilde{S}_n^m(\mathbf{r})}. \tag{48}$$

Certainly, integration of functions preserves the symmetry. Also integrals decorated similarly to the integrand satisfy relations (46) and (47), so for the real basis we have

$$\underline{F}_n^m = \begin{cases} \text{Re} \{ \tilde{F}_n^m \}, & m \geq 0, \\ \text{Im} \{ \tilde{F}_n^m \}, & m < 0 \end{cases} = \begin{cases} \text{Re} \{ \tilde{F}_n^m \}, & m \geq 0, \\ -\text{Im} \{ \tilde{F}_n^{-m} \}, & m < 0 \end{cases}, \quad F = p, q, i, j, a, b. \tag{49}$$

This shows that the complex valued functions can be computed only at non-negative  $m$ .

We have then for the line integrals,

$$\tilde{q}_n^m = \frac{1}{n} [-(\xi_0 + \xi_u) \tilde{q}_{n-1}^{m-1} + (\eta_0 + \eta_u) \tilde{q}_{n-1}^{m+1} - (z_0 + z_u) \tilde{q}_{n-1}^m], \tag{50}$$

$$\tilde{p}_n^m = \frac{1}{n+1} [-\xi_0 \tilde{p}_{n-1}^{m-1} + \eta_0 \tilde{p}_{n-1}^{m+1} - z_0 \tilde{p}_{n-1}^m + \tilde{q}_n^m], \quad m > 0, \quad n = 1, 2, \dots$$

$$\tilde{q}_n^0 = \frac{1}{n} [2 \text{Re} \{ (\eta_0 + \eta_u) \tilde{q}_{n-1}^1 \} - (z_0 + z_u) \tilde{q}_{n-1}^0], \tag{51}$$

$$\tilde{p}_n^0 = \frac{1}{n+1} [2 \text{Re} \{ \eta_0 \tilde{p}_{n-1}^1 \} - z_0 \tilde{p}_{n-1}^0 + \tilde{q}_n^0], \quad n = 1, 2, \dots$$

where for relations at  $m = 0$  we used symmetry (48) and the fact that  $\bar{\xi} = \eta$ .

The surface integrals can be computed using the same recursions for  $\tilde{q}_n^m$  and the following relations for the other quantities

$$\tilde{j}_n^m = \frac{1}{n+1} [-(\xi_0 + \xi_v) \tilde{j}_{n-1}^{m-1} + (\eta_0 + \eta_v) \tilde{j}_{n-1}^{m+1} - (z_0 + z_v) \tilde{j}_{n-1}^m + \tilde{q}_n^m], \tag{52}$$

$$\tilde{i}_n^m = \frac{1}{n+2} (-\xi_0 \tilde{i}_{n-1}^{m-1} + \eta_0 \tilde{i}_{n-1}^{m+1} - z_0 \tilde{i}_{n-1}^m + \tilde{j}_n^m), \quad m > 0, \quad n = 1, 2, \dots$$

$$\begin{aligned}\tilde{j}_n^0 &= \frac{1}{n+1} \left[ 2 \operatorname{Re} \left\{ (\eta_0 + \eta_v) \tilde{j}_{n-1}^1 \right\} - (z_0 + z_v) \tilde{j}_{n-1}^0 + \tilde{q}_n^0 \right], \\ \tilde{i}_n^0 &= \frac{1}{n+2} \left( 2 \operatorname{Re} \left\{ \eta_0 \tilde{i}_{n-1}^1 \right\} - z_0 \tilde{i}_{n-1}^0 + \tilde{j}_n^0 \right), \quad n = 1, 2, \dots\end{aligned}\tag{53}$$

The volume integrals can be computed using the same relations for  $\tilde{q}_n^m$  and  $\tilde{j}_n^m$  and the following relations for the other quantities

$$\begin{aligned}\tilde{b}_n^m &= \frac{1}{n+2} \left[ -(\xi_0 + \xi_w) \tilde{b}_{n-1}^{m-1} + (\eta_0 + \eta_w) \tilde{b}_{n-1}^{m+1} - (z_0 + z_w) \tilde{b}_{n-1}^m + \tilde{j}_n^m \right], \\ \tilde{a}_n^m &= \frac{1}{n+3} \left( -\xi_0 \tilde{a}_{n-1}^{m-1} + \eta_0 \tilde{a}_{n-1}^{m+1} - z_0 \tilde{a}_{n-1}^m + \tilde{b}_n^m \right), \quad m > 0, \quad n = 1, 2, \dots\end{aligned}\tag{54}$$

$$\begin{aligned}\tilde{b}_n^0 &= \frac{1}{n+2} \left[ 2 \operatorname{Re} \left\{ (\eta_0 + \eta_w) \tilde{b}_{n-1}^1 \right\} - (z_0 + z_w) \tilde{b}_{n-1}^0 + \tilde{j}_n^0 \right], \\ \tilde{a}_n^0 &= \frac{1}{n+3} \left( 2 \operatorname{Re} \left\{ \eta_0 \tilde{a}_{n-1}^1 \right\} - z_0 \tilde{a}_{n-1}^0 + \tilde{b}_n^0 \right), \quad n = 1, 2, \dots\end{aligned}\tag{55}$$

Since  $\tilde{F}_0^0 = F_0^0$ ,  $f = p, q, i, j, a, b$ , the initial values for the recursions are provided by Eq. (42).

Finally, we note that integrals for the double layer potential (20) can be computed within the recursive process for the single layer potential using relations

$$\begin{aligned}\tilde{l}_n^m &= \frac{1}{2} \tilde{i}_{n-1}^{m+1} (n_x - i n_y) - \frac{1}{2} \tilde{i}_{n-1}^{m-1} (n_x + i n_y) - \tilde{i}_{n-1}^m n_z, \quad m > 0, \quad n = 1, 2, \dots \\ \tilde{l}_n^0 &= \operatorname{Re} \left[ \tilde{i}_{n-1}^1 (n_x - i n_y) \right] - \tilde{i}_{n-1}^0 n_z, \quad n = 1, 2, \dots\end{aligned}\tag{56}$$

#### 4. Numerical tests

We conducted several numerical tests to confirm the validity of the obtained formulae and measure the performance.

##### 4.1. Accuracy

Integrals  $L$ ,  $M$ , and  $K$  in equations (2) and (3) can be computed analytically. In the numerical tests we compared the results obtained using analytical expressions and the expansions truncated at different truncation numbers. In all tests the expansion center is fixed at the origin of the reference frame, while the evaluation point is set at the point with coordinates

$$\mathbf{r} = d \left( \frac{\sqrt{3}}{2}, 0, \frac{1}{2} \right),\tag{57}$$

where the distance between the expansion center and the evaluation point,  $d$ , is varying. The center of the simplex is placed at  $\mathbf{r}_c = \left( \frac{\sqrt{3}}{2}, 0, 0 \right)$ , while the simplex vertices of are located on a sphere of radius  $r_t$ :

$$\begin{aligned}\mathbf{x}_1 &= \mathbf{r}_c + r_t (-1, 0, 0), \quad \mathbf{x}_2 = \mathbf{r}_c + r_t (1, 0, 0) \quad (\text{segment}), \\ \mathbf{x}_1 &= \mathbf{r}_c + r_t (1, 0, 0), \quad \mathbf{x}_{2,3} = \mathbf{r}_c + r_t \left( -\frac{1}{2}, \pm \frac{\sqrt{3}}{2}, 0 \right) \quad (\text{triangle}), \\ \mathbf{x}_1 &= \mathbf{r}_c + r_t (1, 0, 0), \quad \mathbf{x}_{2,3} = \mathbf{r}_c + r_t \left( -\frac{1}{3}, -\frac{\sqrt{2}}{3}, \pm \sqrt{\frac{2}{3}} \right), \quad (\text{tetrahedron}), \\ \mathbf{x}_4 &= \mathbf{r}_c + r_t \left( -\frac{1}{3}, \frac{2\sqrt{2}}{3}, 0 \right) \quad (\text{tetrahedron}),\end{aligned}\tag{58}$$

Such location of the vertices is selected as probably the worst possible location (in terms of the length of the multipole expansions) for the FMM, in which case one also should use  $d = 1.5$ . We did some accuracy tests by varying  $r_t$  in range  $r_t \in [0.01, 0.2]$ , but found that the effect of varying of the truncation number  $p$  and  $d$  is much stronger. So, below we presented results for  $r_t = 0.1$ , which is typical for the FMM simulations.

#### 4.1.1. Segment

For the line integral we have

$$\begin{aligned} K &= \frac{1}{4\pi} \int_{\mathbf{x}_1}^{\mathbf{x}_2} \frac{dC(\mathbf{r}')}{|\mathbf{r} - \mathbf{r}'|} \\ &= \frac{1}{4\pi} \int_{-1}^1 \frac{d\xi}{\sqrt{\xi^2 - 4\zeta\xi \cos \alpha + 4\zeta^2}} \\ &= \frac{1}{4\pi} \ln \frac{\sqrt{4\zeta^2 - 4\zeta \cos \alpha + 1} + 1 - 2\zeta \cos \alpha}{\sqrt{4\zeta^2 + 4\zeta \cos \alpha + 1} - 1 - 2\zeta \cos \alpha}. \end{aligned} \quad (59)$$

Here we performed the following transformation of the original integral

$$\begin{aligned} \mathbf{r}' &= \mathbf{r}_0 + \frac{1}{2}\mathbf{p}\xi, \quad \mathbf{r}_0 = \frac{1}{2}(\mathbf{x}_1 + \mathbf{x}_2), \quad \mathbf{p} = \mathbf{x}_2 - \mathbf{x}_1, \\ \xi &\in [-1, 1], \quad dl = \frac{1}{2}J\xi, \quad J = |\mathbf{p}|, \end{aligned} \quad (60)$$

and denoted

$$\zeta = \frac{|\mathbf{r} - \mathbf{r}_0|}{J}, \quad \cos \alpha = \frac{(\mathbf{r} - \mathbf{r}_0) \cdot \mathbf{p}}{|\mathbf{r} - \mathbf{r}_0| J}. \quad (61)$$

Figure 2 shows the relative error,  $\epsilon = |K - K_{an}|/K_{an}$ , where  $K_{an}$  is provided by equations (59)-(61) and  $K$  is computed using the series expansion and the recursive procedure (50)-(51) for the expansion coefficients. It is seen that the error can be reduced to a desired level by a proper selection of parameter  $p$ . The distance  $d$  plays also an important role. Theoretically, the error depends on  $p$  and  $d$  as

$$\epsilon = C \left( \frac{|\mathbf{r}_c - \mathbf{r}_*|}{d} \right)^p, \quad (62)$$

where  $C$  is some constant, since the series can be majorated by a geometric progression. We plotted these curves on Fig. 2 at  $C = 0.1$  and different fixed values of  $\epsilon$ . It is seen that the computed error is consistent with the theoretical error bound.

#### 4.1.2. Triangle

While analytical expressions for integrals for flat quadrilaterals can be found in [11] and can be modified for triangles, we can obtain analytical expressions by reduction of the surface integrals to the contour integrals using the Gauss divergence theorem and then by evaluating the integrals over the segments using the

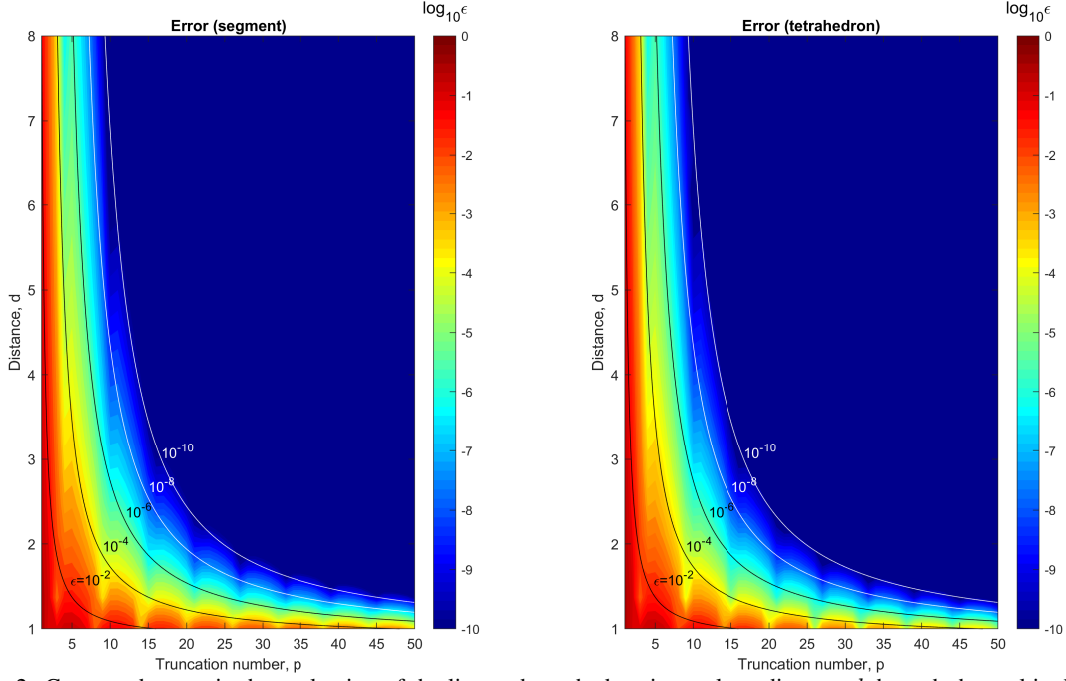


Figure 2: Computed errors in the evaluation of the line and tetrahedron integrals at distance  $d$  through the multipole expansions derived for various values of the truncation number  $p$ . The lines show the theoretical error levels according to Eq. (62).

primitives. Below we display only the final expressions [4] needed for validation of the obtained recursions.

$$\begin{aligned}
 L(\mathbf{r}) &= \int_S G(\mathbf{r}, \mathbf{r}') dS(\mathbf{r}') = \frac{1}{4\pi} \sum_{q=1}^3 [L_P(l_q - x_q, h, z_q) - L_P(-x_q, h, z_q)], \quad (63) \\
 M(\mathbf{r}) &= \int_S \frac{\partial G(\mathbf{r}, \mathbf{r}')}{\partial n(\mathbf{r}')} dS(\mathbf{r}') = \frac{1}{4\pi} \sum_{q=1}^3 [M_P(l_q - x_q, h, z_q) - M_P(-x_q, h, z_q)], \\
 x_q &= (\mathbf{r} - \mathbf{x}_q) \cdot \mathbf{i}_q, \quad h = |(\mathbf{r} - \mathbf{x}_1) \cdot \mathbf{n}|, \quad z_q = (\mathbf{r} - \mathbf{x}_q) \cdot \mathbf{n}_q, \\
 \mathbf{i}_q &= \frac{1}{l_q} (\mathbf{r}_{q(\text{mod } 3)+1} - \mathbf{x}_q), \quad l_q = |\mathbf{x}_{q(\text{mod } N_e)+1} - \mathbf{x}_q|, \quad \mathbf{n}_q = \mathbf{i}_q \times \mathbf{n}, \\
 L_P(x, y, z) &= -yM_P(x, y, z) - z \ln|r + x|, \quad M_P(x, y, z) = -\arctan \frac{xz(r - y)}{rz^2 + yx^2}, \\
 r &= \sqrt{x^2 + y^2 + z^2}.
 \end{aligned}$$

Figure 3 shows the relative errors between the analytical solutions and  $L$  and  $M$  computed using the series expansion and the recursive procedure (52)-(56) for the expansion coefficients. Note that while the error for the single layer potential can be described by Eq. (62), the error of the double layer potential can be estimated as

$$\epsilon = Cp \left( \frac{|\mathbf{r}_c - \mathbf{r}_*|}{d} \right)^{p-1}, \quad (64)$$

with the same constant  $C$  as for the single layer. This relation is obtained by estimation of the residual of the derivative of the geometric progression majorating the single layer potential. We plotted curves described

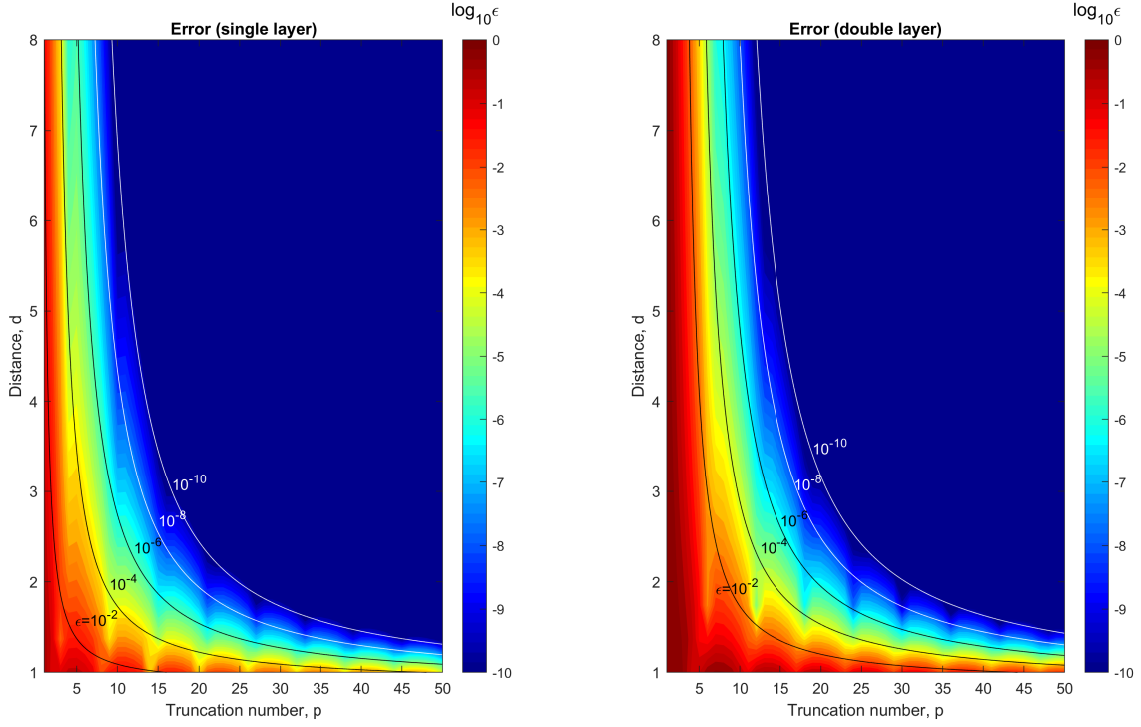


Figure 3: Error in the evaluation of the single layer and double layer integrals over a boundary triangle at distance  $d$  through the multipole expansions derived for various values of the truncation number  $p$ . The lines show the theoretical error levels according to Eqs (62) and (64).

by Eqs (62) and (64) on Fig. 3 at  $C = 0.1$  and different fixed values of  $\epsilon$ . It is seen that the computed error is consistent with the theoretical error bound.

#### 4.1.3. Tetrahedron

Analytical expression for tetrahedrons, can be obtained from those for flat triangles. Indeed, we have according to the Gauss divergence theorem

$$\begin{aligned}
 N(\mathbf{r}) &= \int_V G(\mathbf{r}, \mathbf{r}') dV(\mathbf{r}') = -\frac{1}{2} \int_V \nabla_{\mathbf{r}'} \cdot [(\mathbf{r} - \mathbf{r}') G(\mathbf{r}, \mathbf{r}')] dV(\mathbf{r}') \\
 &= -\frac{1}{2} \int_S \mathbf{n}(\mathbf{r}') \cdot [(\mathbf{r} - \mathbf{r}') G(\mathbf{r}, \mathbf{r}')] dS(\mathbf{r}') = -\frac{1}{2} \sum_{j=1}^4 \int_{S_j} \mathbf{n}_j \cdot (\mathbf{r} - \mathbf{r}') G(\mathbf{r}, \mathbf{r}') dS(\mathbf{r}'),
 \end{aligned} \tag{65}$$

where  $S_j$  are the faces of tetrahedron  $V$  and  $\mathbf{n}_j$  are the normals to the faces directed outside the tetrahedron. Denoting  $\mathbf{r}_{cj}$  the centers of the faces, and noticing that  $\mathbf{n}_j \cdot (\mathbf{r}' - \mathbf{r}_{cj}) = 0$ , we obtain

$$\begin{aligned}
 N(\mathbf{r}) &= -\frac{1}{2} \sum_{j=1}^4 \int_{S_j} \mathbf{n}_j \cdot (\mathbf{r} - \mathbf{r}_{cj} - (\mathbf{r}' - \mathbf{r}_{cj})) G(\mathbf{r}, \mathbf{r}') dS(\mathbf{r}') \\
 &= -\frac{1}{2} \sum_{j=1}^4 \mathbf{n}_j \cdot (\mathbf{r} - \mathbf{r}_{cj}) \int_{S_j} G(\mathbf{r}, \mathbf{r}') dS(\mathbf{r}') = -\frac{1}{2} \sum_{j=1}^4 \mathbf{n}_j \cdot (\mathbf{r} - \mathbf{r}_{cj}) L_j(\mathbf{r}).
 \end{aligned} \tag{66}$$



Here the single layer potential  $L_j(\mathbf{r})$  can be computed using Eq. (63).

Figure 2 shows the errors for the integral over the tetrahedron. The theoretical error bound here is provided by Eq. (62) and plotted in the figure for  $C = 0.1$  and different fixed values of  $\epsilon$ . It is seen that the computed error is consistent with the theoretical error bound. Also, they agree well with the errors for the line segment, which has the same bound.

## 4.2. Performance

### 4.2.1. Gauss quadrature

Expansion coefficients  $K_n^m$ ,  $L_n^m$ , and  $M_n^m$  can be computed exactly using quadrature formulae, such as the Gauss-Legendre quadrature. Indeed the basis functions  $R_n^m$  are polynomials of degree  $n$ , so, it is sufficient to use the Gauss quadrature of the order of  $(n + 1)/2$  (take the ceiling if this number is not integer). For triangles special quadrature formulae of this type can be derived. However, as soon as the integral can be transformed to the integral over a standard triangles, which can be represented by a double integral, the Gauss quadrature can be applied to each integral.

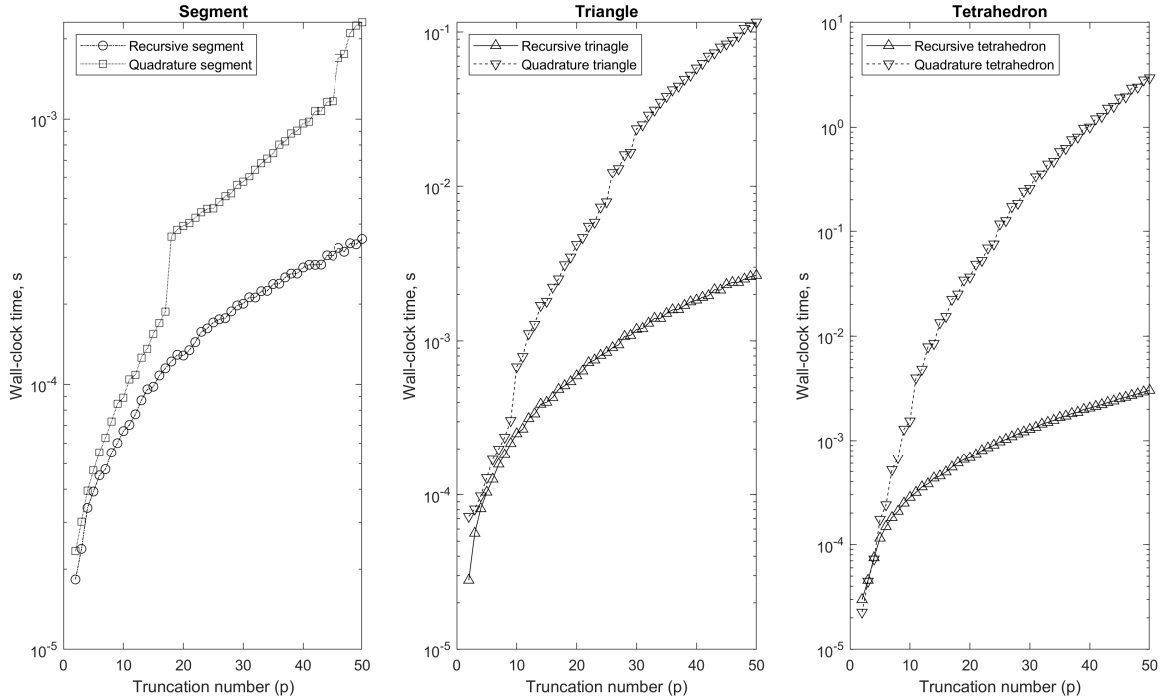


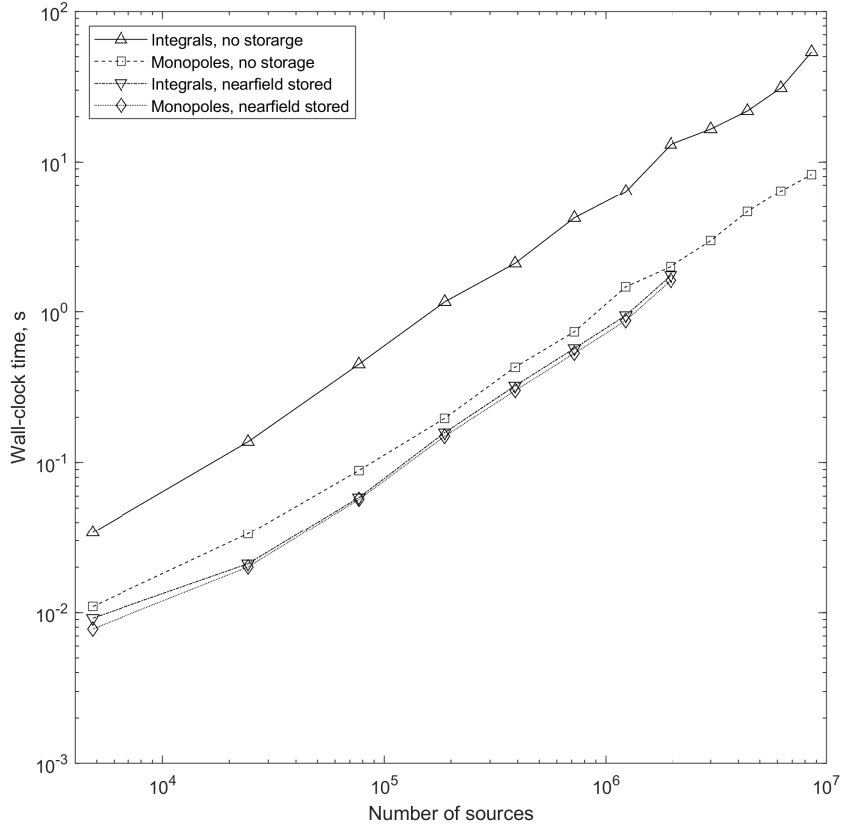
Figure 4: The wall-clock times (for Matlab function prototypes) for computation of the multipole expansions for uniform charge distributions over a line segment, triangle, and tetrahedron. Two methods are compared for each case: the present method (recursive) and the method based on the Gauss quadrature with the number of nodes providing exact integration of the polynomials of degree  $p$ . The difference between the results of the two methods are within the round-off errors for double precision arithmetic. A significant speedup is seen.

First, we compared the results obtained using the present recursive processes and those obtained using the numerical quadrature and confirmed that the difference is of the order of the round-off errors for double precision computing. Second, we measured the time to generate multipole expansion using the quadrature formulae and the recursions. These tests were performed using Matlab, where the quadrature results were computed using vectorization, while the recursions were obtained in a serial manner (loop) for the increasing  $n$ . For quadrature, all  $R_n^m$  at the quadrature nodes were computed recursively from  $n = 0$  to a given  $p - 1$ .

using recursions for  $k_n^m$  (see Eqs (40) and (41)) and then summation was performed using precomputed quadrature weights. Even though the quadrature formulae are computed using vectorization, Fig. 4 shows that the present recursive process outperforms the method based on the quadrature. This is clearly seen for the segment, where the wall clock time can be several time smaller for the recursive method. The effect is much stronger for the triangle, where the present process can be 1-2 orders of magnitude faster than the quadrature computations. It is even stronger for the tetrahedron when the recursive computations can be 3 orders of magnitude faster compared to the quadrature method. Of course, the acceleration of computations depends on the truncation number, and for small truncation numbers the benefit is not so great. But anyway, in all cases we tried we observed that the recursive method is faster.

#### 4.2.2. Fast multipole method

For illustrations we considered two example computations using the FMM. The times were obtained on a work station equipped with Intel Xeon CPU processors at 2.1 GHz with total 32 physical cores and 128 GB RAM using an Open MP parallelized code without GPU as described in [7].



6

Figure 5: Comparisons of the wall-clock time performance of the FMM used for summation of monopoles distributed at the triangle centers over the surface of some object and summation of single layer integrals for the same surface covered by triangles. Performance for two options is shown: with and without storage of the nearfield interaction sums (with optimized octree depth for each case). The difference in computation times for the option with storage relates only to the speed of generation of multipole expansions. Times are measured for a 32 core Intel Xeon CPU with a clock speed of 2.1 GHz and 128 GB RAM. The penalty for accurate consistent quadrature is seen to be minimal.

In the first example, we computed the single layer potential  $L$  for a unit sphere with a random distribution

of the charge density. The recursive computations of the multipole expansions were implemented and the performance was compared with summation of monopoles for the same source and receiver locations (at the triangle centers). The reason for such test is to see how much the FMM slows down, due to the computation of integrals. Note here, that the FMM can be optimized in terms of performance by appropriate selection of the clustering parameter,  $s$ , (which is the maximum number of sources in a box at the maximum level of the octree; this parameter controls the depth of the octree) (e.g., see [7]) and we report only data for the optimized cases. We also note that the matrix for nearfield interactions (a sparse matrix) in the FMM can be computed “on the fly” every time when the matrix-vector product is needed or it can be computed and stored. The latter method is preferable for iterative solutions of large systems, as only the input vector is changing in such a process, while the matrix does not change. The former method is preferable when only one or very few evaluations are needed (e.g., for evaluation of the integrals with already known charge density at some field points). Sometimes one is forced to use this method even for iterative computations if there are not enough memory to store the nearfield interaction matrix.

By this reason we considered two cases for comparisons shown in Fig. 5. In all cases the truncation number was  $p = 10$ , which provides the overall relative  $L_2$ -error of the FMM of the order of  $\epsilon_2 \sim 10^{-6}$  (see also [7]). In all cases the error was the same for the monopole summation and for summation of the integrals over triangles. “On the fly” computing of the nearfield interaction shows that the runtime for the monopole summation ( $s = 300$ ) is about 3-6 times smaller than for summation of integrals ( $s = 30$ ). However, for the case when the nearfield matrices are precomputed and stored the monopole summation ( $s = 400$ ) is only 3-17% faster than that for the integrals ( $s = 400$ ). Note that in this case the entire difference in performance of the code for monopoles and triangles is due to the multipole expansions, as all other steps of the algorithm are the same. A big difference in the performance when the nearfield interactions are computed directly is only due to direct computation of integrals (63), which is much more arithmetically intensive than computation of the Green function.

In the second example, we modified the FMM-accelerated vortex filament method (see [8]) with a recursive process described in the present paper. The wall clock time was measured for different number of elementary vortex filaments randomly distributed in space and compared with the times obtained when the multipole expansions of line integrals are computed using the Gauss quadrature. Figure 6 shows the results for truncation number  $p = 34$  and  $s = 600$ . In all cases the use of the recursive integral computations showed acceleration, which for the results plotted varied in the range 20-40%.

## 5. Conclusions

The method for recursive computation of the multipole expansions of the single and double potentials of the triangles and potentials of the segments and tetrahedrons is developed and tested. The tests show consistency of the results with analytical expressions and numerical integration using quadrature formulae of appropriate order. In all cases considered the developed process shows better performance than other methods.

According to our tests using an FMM code, the performance of the method for summation of integrals based on the present method of generation of multipole expansions is only 3-17% slower than summation of multipoles (the fastest process for the FMM) in the case when the nearfield interaction matrix is precomputed and stored. The use of the recursive process may increase the performance of the vortex filament codes up to 40%.

It is remarkable that the present method can be also used in computations of the Galerkin integrals (e.g., see [2]). Indeed, the no-touch cases can be computed using the multipole expansions. Furthermore, if the Galerkin method is used with the FMM, the far field interactions are locally represented by series over

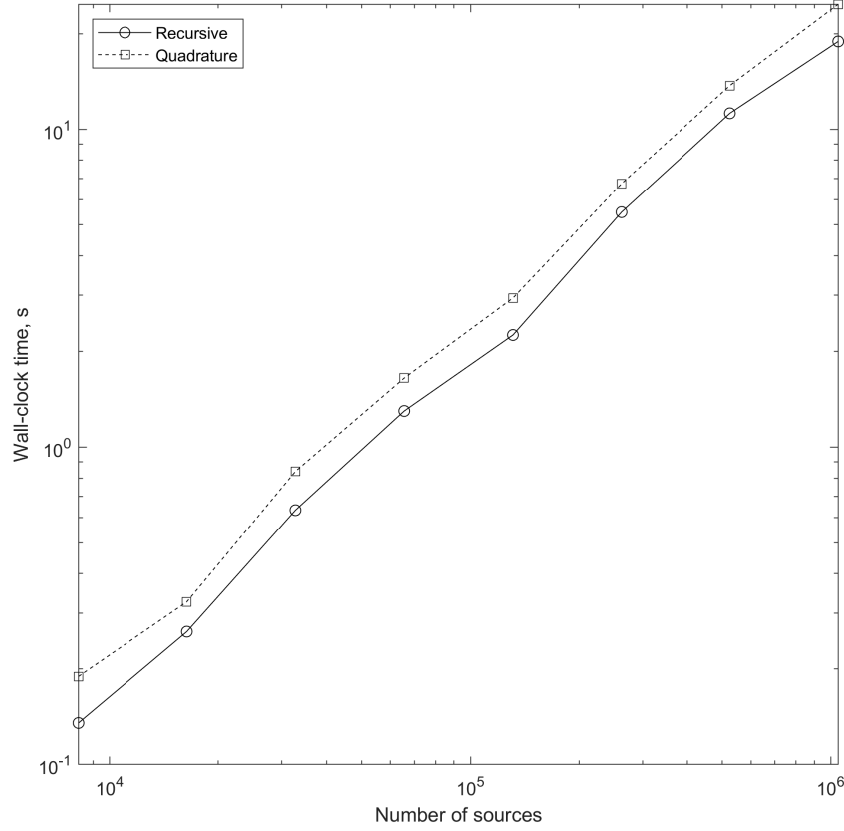


Figure 6: The wall-clock times for the FMM accelerated vortex filament method (truncation number  $p = 34$ , clustering parameter,  $s = 600$ , just summation) with recursive computation of multipole expansions and computations of the same expansion using the Gauss quadrature. Times are measured for the same workstation as in Fig. 5. A consistent significant speedup is observed.

functions  $R_n^m(\mathbf{r})$ , which should be integrated over the receiving triangles. In this case we have exactly the case considered in the present paper and the fast recursive evaluation of the integrals can be applied here as well.

## 6. Acknowledgments

This work is supported by Cooperative Research Agreement (W911NF1420118) between the University of Maryland and the Army Research Laboratory, with David Hull, Ross Adelman and Steven Vinci as Technical monitors.

## References

- [1] ABRAMOWITZ, MILTON, STEGUN, IRENE A, & ROMER, ROBERT H. 1988. Handbook of Mathematical Functions with Formulas, Graphs, and Mathematical Tables. *Am. J. Phys.*, **56**(10), 958–958.
- [2] ADELMAN, R, GUMEROV, N A, & DURAISWAMI, R. 2016. Computation of Galerkin double surface integrals in the 3-D boundary element method. *IEEE Transactions on Antennas and Propagation*.

- [3] ADELMAN, R, GUMEROV, N A, & DURAI SWAMI, R. 2017. FMM/GPU-Accelerated Boundary Element Method for Computational Magnetism and Electrostatics. *IEEE Trans. Magn.*, **53**(12), 1–11.
- [4] ADELMAN, ROSS. 2016. *Fast and accurate boundary element methods in three dimensions*. Ph.D. thesis, University of Maryland, College Park.
- [5] GREENGARD, L, & ROKHLIN, V. 1987. A fast algorithm for particle simulations. *J. Comput. Phys.*, **73**(2), 325–348.
- [6] GUMEROV, N A, & DURAI SWAMI, R. 2006. Fast multipole method for the biharmonic equation in three dimensions. *J. Comput. Phys.*
- [7] GUMEROV, N A, & DURAI SWAMI, R. 2008. Fast multipole methods on graphics processors. *J. Comput. Phys.*
- [8] GUMEROV, N A, & DURAI SWAMI, R. 2013. Efficient FMM accelerated vortex methods in three dimensions via the Lamb–Helmholtz decomposition. *J. Comput. Phys.*
- [9] GUMEROV, N A, ADELMAN, R N, & DURAI SWAMI, R. 2020. Boundary Element Solution of Electromagnetic Fields for Non-Perfect Conductors at Low Frequencies and Thin Skin Depths. *IEEE Trans. Magn.*, **56**(11), 1–12.
- [10] HARRINGTON, R F. 1987. The Method of Moments in Electromagnetics. *Journal of Electromagnetic Waves and Applications*, **1**(3), 181–200.
- [11] HESS, J L, & SMITH, A M O. 1967. Calculation of potential flow about arbitrary bodies. *Prog. Aerosp. Sci.*, **8**, 1–138.
- [12] NISHIMURA, N. 2002. *Fast multipole accelerated boundary integral equation methods*.
- [13] NISHIMURA, NAOSHI, YOSHIDA, KEN-ICHI, & KOBAYASHI, SHOICHI. 1999. A fast multipole boundary integral equation method for crack problems in 3D. *Eng. Anal. Bound. Elem.*, **23**(1), 97–105.
- [14] OF, G, STEINBACH, O, & WENDLAND, W L. 2005. Applications of a fast multipole Galerkin in boundary element method in linear elastostatics. *Comput. Vis. Sci.*, **8**(3), 201–209.
- [15] WANG, HAITAO, LEI, TING, LI, JIN, HUANG, JINGFANG, & YAO, ZHENHAN. 2007. A parallel fast multipole accelerated integral equation scheme for 3D Stokes equations. *Int. J. Numer. Methods Eng.*, **70**(7), 812–839.